Published in final edited form as:
J Biol Chem. 2006 February 17; 281(7): 4222–4230. doi:10.1074/jbc.M509769200.

Light-induced Oxidation of Photoreceptor Outer Segment Phospholipids Generates Ligands for CD36-mediated Phagocytosis by Retinal Pigment Epithelium:

A Potential Mechanism for Modulating Outer Segment Phagocytosis Under Oxidant Stress Conditions*

Mingjiang Sun[‡,§], **Silvia C. Finnemann**[¶,1], **Maria Febbraio**[§], **Lian Shan**[§], **Suresh P. Annangudi**[‡], **Eugene A. Podrez**[§], **George Hoppe**[‖], **Ruth Darrow**[**], **Daniel T. Organisciak**[**], **Robert G. Salomon**[‡], **Roy L. Silverstein**[§], and **Stanley L. Hazen**[§,‡‡,2]

[‡]Department of Chemistry, Case Western Reserve University, Cleveland, Cleveland, Ohio 44106

[§]Department of Cell Biology, Cleveland Clinic Foundation, Cleveland, Ohio 44195

[‡‡]Department of Cardiovascular Medicine and the Center for Cardiovascular Diagnostics and Prevention, Cleveland Clinic Foundation, Cleveland, Ohio 44195

[¶]Department of Dyson Vision Research Institute, Department of Ophthalmology, Department of Cell and Developmental Biology, and Department of Physiology and Biophysics, Weill Medical College of Cornell University, New York, New York 10021

[‖]Department of Cole Eye Institute, Cleveland Clinic Foundation, Cleveland, Ohio 44195

[**]Department of Biochemistry and Molecular Biology, Wright State University School of Medicine, Dayton, Ohio 45401-0927

Abstract

Clearance by the retinal pigment epithelium (RPE) of shed photoreceptor outer segments (OSs), a tissue with one of the highest turnover rates in the body, is critical to the maintenance and normal function of the retina. We hypothesized that there is a potential role for photo-oxidation in OS uptake by RPE via scavenger receptor-mediated recognition of structurally defined lipid peroxidation products. We now demonstrate that specific structurally defined oxidized species derived from arachidonyl, linoleoyl, and docosahexanoyl phosphatidylcholine may serve as endogenous ligands on OSs for uptake by RPE via the scavenger receptor CD36. Mass spectrometry studies of retinal lipids recovered from dark-adapted rats following physiological light exposure demonstrate *in vivo* formation of specific oxidized phosphatidylcholine molecular species possessing a CD36 recognition motif, an oxidatively truncated *sn*-2 acyl group with a terminal γ-hydroxy(or oxo)-α,β-unsaturated carbonyl. Cellular studies using RPE isolated from wild-type *versus* CD36 null mice suggest that CD36 plays a role in engulfment, but not initial binding, of OSs via these oxidized phospholipids. Parallel increases in OS protein-bound nitrotyrosine, a post-translational modification by nitric oxide (NO)-derived oxidants, were also

*This work was supported in part by National Institutes of Health Grants P01 HL076491, P01 HL77107, HL70621, HL61878, EY10967, HL46403, EY13295, and EY01959 and by the Cleveland Clinic Foundation General Clinical Research Center (Grant M01 RR018390). The costs of publication of this article were defrayed in part by the payment of page charges. This article must therefore be hereby marked *"advertisement"* in accordance with 18 U.S.C. Section 1734 solely to indicate this fact.

[2]To whom correspondence should be addressed: Center for Cardiovascular Diagnosticsand Prevention, Cleveland Clinic Foundation, 9500 Euclid Ave., NE-10, Cleveland, OH 44195. Tel.: 216-445-9763; Fax: 216-636-0392; hazens@ccf.org.
[1]The Research To Prevent Blindness William & Mary Greve Scholar and the recipient of an Irma T. Hirschl Career Scientist Award.

observed, suggesting a possible role for light-induced generation of NO-derived oxidants in the initiation of OS lipid peroxidation. Collectively, these studies suggest that intense light exposure promotes “oxidative tagging” of photoreceptor outer segments with structurally defined choline glycerophospholipids that may serve as a physiological signal for CD36-mediated phagocytosis under oxidant stress conditions.

Shedding and clearance of effete photoreceptor rod outer segments (OSs)[*3] are critical for maintenance of normal retinal function. New disks are constantly generated at the basal end of OS disk stacks, and old disks then shed from the apical tip where they are digested by phagocytic retinal pigment epithelium (RPE). Shedding is believed to occur because OSs are routinely damaged, possibly by oxidative modifications spawned by photo-generated radicals (1, 2). For example, albino rats reared in cyclic light demonstrate a burst of retinal OS disk shedding soon after the onset of light, with the number of large packets of OSs in RPE substantially greater than at any other time of day or night, suggesting that light damage triggers OS phagocytosis by RPE (2). OSs are rich in unsaturated lipids, especially docosahexaenoic acid (DHA). The presence of six allylic groups within DHA renders this highly unsaturated fatty acid exquisitely sensitive to oxidation, a process likely further facilitated by the localized oxygen and light-rich environment of the retina (3). Phagosomes arising from OS shedding have been shown to increase dramatically in RPE of rats exposed to intense light in intermittent light/dark cycles, whereas ascorbate treatment has been shown to prevent the accumulation of phagosomes (4). Thus, it is reasonable to hypothesize that oxidative modification of OSs may occur in the retina and that phospholipid peroxidation products may serve as signaling molecules for RPE phagocytosis (5).

Phagocytosis of OSs by the RPE is a receptor-mediated process (1) involving at least two independent steps. Shed OSs initiate a signaling pathway within RPE via the integrin $\alpha v\beta 5$ (6, 7), activating phagocytic machinery for OS internalization that requires the receptor tyrosine kinase Mer (8–12). *In vitro* data suggest that other RPE surface receptors, such as the class B scavenger receptor CD36 (13) and the mannose receptor (14), are also involved in phagocytosis of OSs by the RPE. Blocking CD36 by either anionic phospholipids or CD36 antibody partially inhibits OS uptake by RPE *in vitro* (15), and ligation of CD36 appears to serve a signaling function in RPE leading to enhanced uptake of OSs (16). The nature of ligands on OSs recognized by phagocytic receptors, including CD36, remains undefined.

CD36 is a heavily glycosylated, single chain, integral plasma membrane protein that belongs to an evolutionarily conserved family of proteins that serve as scavenger and lipid receptors (17,18). It is expressed on the surface of adipocytes, microvascular endothelial cells, macrophages, dendritic cells, platelets, and specialized epithelial cells, such as RPE (17, 18). CD36 functions *in vivo* in scavenger recognition of oxidized lipoproteins and apoptotic

[3]The abbreviations used are: OS, rod outer segment; A-PC, G-PC, and S-PC, azeleic acid, glutaric acid, and succinic acid esters of 2-lyso-PC; DHA-PC, PA-PC, PL-PC, and POPC, the docosahexaenoic acid, arachidonic acid, linoleic acid, and oleic acid esters of 2-lyso-PC; DTPA, diethylenetriaminepentaacetic acid; DTPC, 1,2-ditridecanoyl-*sn*-glycero-3-phosphatidylcholine; FITC, fluorescein isothiocyanate; HDdiA-PC, HdiA-PC, and HOdiA-PC, the 9-hydroxy-11-carboxyundec-6-enoic acid, 4-hydroxy-7-carboxy-hex-5-enoic acid, and 7-carboxy-5-hydroxyhept-6-enoic acid esters of 2-lyso-PC; HODA-PC, HOHA-PC, and HOOA-PC, the 9-hydroxy-12-oxododec-10-enoic acid, 4-hydroxy-7-oxohept-5-enoic acid, and 5-hydroxy-8-oxoocta-6-enoic acid esters of 2-lyso-PC; HPLC, high performance liquid chromatography; [^{125}I]NO_2-LDL, ^{125}I-la-beled low density lipoproteins modified by the myeloperoxidase-hydrogen peroxide-nitrite system; KHdiA-PC, KOdiA-PC, and KDdiA-PC, the 6-carboxy-4-oxohex-5-enoic acid and 7-carboxy-5-oxohept-6-enoyl- and 11-carboxyl-9-oxoundec-6-enoic acid esters of 2-lyso-PC; KODA-PC, KOHA-PC, and KOOA-PC, the 9,12-dioxododec-10-enoic acid, 4,7-dioxohept-6-enoic acid, and 5,8-dioxooct-6-enoic acid esters of 2-lyso-PC; KO, knockout; LC, liquid chromatography; lyso-PC, 1-palmitoyl-2-hydroxy-*sn*-glycero-3-phosphatidylcholine; MS, mass spectrometry; MPO, myeloperoxidase; OB-PC, ON-PC, and OV-PC, the 4-oxobutyric acid, 9-oxononanoic acid, and 5-oxova-leric acid esters of 2-lyso-PC; $oxPC_{CD36}$, oxPC that bind to the scavenger receptor CD36; oxLDL, oxidized low density lipoprotein; oxPC, oxidized phosphatidylcholine molecular species; oxPL, oxidized phospholipids; RPE, retina pigment epithelial cells; WT, wild-type; DMEM, Dulbecco's modified Eagle's medium; FITC, fluorescein isothiocyanate.

cells, fatty acid transport, and cell-matrix interactions (19–21). Recent studies have focused on CD36 as a participant in the atherosclerotic process because of its ability to recognize oxidized forms of LDL (17, 19, 22, 23). CD36 mediates lipid accumulation and macrophage foam cell formation *in vitro* and *in vivo* (22) and atherosclerosis-prone apoE null mice were markedly protected from developing atherosclerotic lesions when bred into a CD36 null background (21).

In recent studies we identified a novel family of structurally specific oxidized phosphatidylcholine molecular species (oxPCs) derived from 1-palmitoyl-2-linoleoyl-*sn*-glycero-3-phosphatidylcholine (PLPC) and 1-palmitoyl-2-arachidonoyl-sn-glycero-3-phosphatidylcholine(PAPC) that serve as high affinity ligands for CD36 ($oxPC_{CD36}$). Synthetic methods for generation of individual $oxPC_{CD36}$ were developed (24), and then these species were shown to selectively inhibit the binding of oxLDL to CD36-transfected cells. Vesicles containing low mole % of synthetic $oxPC_{CD36}$ were also shown to be taken up by cells via CD36 (24, 25). A common structural motif for all $oxPC_{CD36}$ species was identified as an oxidatively truncated *sn*-2 acyl group with a terminal γ-hydroxy(or oxo)-α,β-unsaturated carbonyl (Fig. 1A). Mass spectrometry analyses revealed that $oxPC_{CD36}$ are generated by a variety of oxidation processes and are enriched in atherosclerotic plaques (26).

The phospholipid content of retina is markedly enriched in docosahexaenoic acid (22:6), a highly unsaturated fatty acid whose complex oxidation products are relatively poorly described. High levels of carboxyethylpyrrole modifications of proteins are observed in retinas of individuals with age-related macular degeneration, providing presumptive evidence for the generation of docosahexaenoate-derived oxidatively truncated phospholipids in retinal pathology (27). Based upon known mechanisms of lipid peroxidation, we recently generated a family of presumed oxidation products of the docosahexaenoate ester of 2-lysophosphatidylcholine (DHA-PC) by total syntheses, and then confirmed their formation by free radical-induced oxidative cleavage of DHA-PC *in vitro* (28).

We hypothesized that $oxPC_{CD36}$ derived from DHA-PC are generated on OSs as a consequence of oxidative stress, such as with light exposure, and that these oxidized choline glycerophospholipids might serve as a physiological signal to facilitate OS phagocytosis by RPE via CD36. Herein we structurally identify specific oxPCs derived from DHA-PC photo-oxidation and further show that $oxPC_{CD36}$ derived from DHA-PC, PAPC, and PLPC and their down-stream oxidation products, are produced *in vivo* within the retina of dark-adapted rats following intense light exposure. Finally, using RPE isolated from CD36 knock-out mice, we demonstrate that RPE-mediated internalization of OSs is facilitated via CD36-specific interaction with $oxPC_{CD36}$. Our findings suggest that light-induced oxidation of retinal OSs phospholipids such as DHA-PC may serve as a physiological “eat me” signal for CD36-mediated phagocytosis by RPE.

Experimental Procedures

Materials

$Na^{125}I$ was supplied by ICN Pharmaceutical, Inc. PLPC, PAPC, DHA-PC, 1,2-ditridecanoyl-*sn*-glycero-3-phosphatidylcholine (DTPC), 1-palmitoyl-2-hydroxy-*sn*-glycero-3-phosphatidylcholine (lyso-PC), and 1-palmitoyl-2-oleoyl-sn-glycero-3-phosphatidylcholine (POPC), were obtained from Avanti Polar Lipids Inc. (Alabaster, AL). Synthetic oxPCs were prepared as previously described (24, 28, 29). LDL was prepared from human plasma and oxidized by exposure to leukocyte myeloperoxidase in the presence

of nitrite as previously described (22). Other chemicals were obtained from Sigma unless specified.

Photo-oxidation of DHA-PC

DHA-PC (1 mg) was hydrated at 37 °C for 1 h in argon-sparged phosphate buffer (1 ml) supplemented with DTPA to minimize transition metal-induced auto-oxidation. The hydrated DHA-PC were then made into unilamellar vesicles by extrusion using an Avanti Mini-Extruder (Avanti Polar Lipids, Inc). The vesicles (400 μl) were kept in the dark under argon blanket at room temperature until use the same day. Photo-oxidation was performed by transfer of vesicles into a quartz tube placed in the center of a Rayonet photochemical reactor with three 80-watt low pressure mercury UV (254 or 350 nm) lamps (Southern New England Ultraviolet, Midtown, CT). Reaction mixtures were incubated in air with temperature maintained at 28 °C. Sampling (30 μl) was performed at various times, and the reaction was stopped by adding catalase (10 μl and 150 μM final) and butylated hydroxytoluene (2 μl and 40 μM final). For quantification purposes, lipid extraction was performed immediately after addition of DTPC (300 ng) using the method of Bligh and Dyer (30). Extracts were dried under N_2 and stored in vials sealed under argon at −80 °C until analysis.

Mass Spectrometric Analysis of Light-irradiated DHA-PC

Mass spectrometric analyses of irradiated DHA-PC was performed on an ABI 365 mass spectrometer equipped with Ionics EP 10+ upgrade (Concord, Ontario, Canada), interfaced with a Waters 2790 (Waters, Milford, MA) HPLC system. Oxidized DHA-PC (30 μg) was dissolved in 1 ml of methanol. The solution (10 μl) was diluted with 140 μl of methanol containing 10% water. This solution (50 μl) was chromatographed on a Prodigy ODS C18 column (150 × 2 mm, 5 μm, Phenomenex, Torrance, CA) with a binary solvent gradient, starting from 100% water for the first 5 min, then a linear gradient to 100% methanol in 15 min, and then 100% methanol for 20 min, at a flow rate of 0.2 ml/min. All mobile phase solvents contained 0.2% formic acid. The total ion current was obtained in the mass range of m/z 200–1000 using a cone energy of 30 V in the positive ion mode. Three kV was applied to the electrospray capillary.

Characterization of DHA-PC Oxidation Products as CD36 Ligands

Specific binding of synthetic oxPC species were determined in competition binding assays employing ^{125}I-labeled LDL exposed to the myeloperoxidase/H_2O_2/ NO_2^- system ([^{125}I]NO_2LDL) and CD36 cDNA-transfected 293 cells, as previously described (25). Presentation of the individual oxPC was normalized by incorporation as a low mol % component (10%) of vesicles generated with POPC as carrier (25). CD36 independent binding of [^{125}I]NO_2LDL was assessed in control vector-transfected 293 cells and subtracted from binding to CD36-transfected 293 cells, whose binding was typically <10–20% that of CD36-transfected cells. Each measurement was performed in triplicate, and results shown represent averages from at least three independent experiments.

RPE Cells

An SV40-transformed cell line derived from rat RPE, RPE-J cells, has been previously characterized and is frequently used to study phagocytic function (31). These cells were routinely maintained at 32 °C in DMEM supplemented with 4% fetal calf serum. Cells were seeded at 50% confluence on 5-mm glass coverslips in 96-well plates and grown for 6–7 days before use at a density of 3.3×10^5 cells/well. Under these conditions, RPE-J cells possess epithelial morphology and apical expression of phagocytic proteins $\alpha v\beta 5$ and MerTK (32). Where indicated, primary RPE cells were used. These were obtained from both

CD36 null mice and wild-type C57Bl/6 controls. CD36 nulls were backcrossed seven times onto a C57Bl background. Mice were sacrificed by CO_2 asphyxiation at 12–14 days of age. Following eyeball enucleation and removal of cornea, iris, lens, and vitreous, eyecups were incubated in 1 mg/ml hyaluronidase in Ca^{2+} and Mg^{2+}-free Hanks' buffered saline solution to detach neural retinas from the underlying RPE. A circumferential cut was made just below the ora serrata to remove neural retinas from eyecups. Eyecups with exposed RPE apical surface were further incubated in 2 mg/ml trypsin in Hanks' buffered saline solution containing Ca^{2+} and Mg^{2+} for 45 min at 37 °C. Sheets of RPE were peeled off Bruch's membrane, trypsinized, pelleted, resuspended, and seeded as patches in DMEM supplemented with 10% fetal calf serum. Primary RPE cells were routinely used 4–7 days after preparation. To characterize epithelial morphology, we fixed samples with ice-cold methanol and labeled nuclei with 1 μg/ml propidium iodide and tight junctions with ZO-1 antibodies (Zymed Laboratories Inc.) and secondary alexa488-conjugated antibodies (Molecular Probes). Laser scanning confocal microscopy using a Leica TSP2 system revealed no significant difference in yield, attachment, spreading, or pigmentation of RPE derived from CD36 null compared with wild-type controls.

OS Phagocytosis Assays by RPE Cells

OSs were isolated on 25–60% sucrose gradients from fresh bovine retinas according to established protocols (32) and labeled with fluorescein isothiocyanate (FITC, Molecular Probes, Eugene, OR) as previously described (7). RPE cells on 5-mm coverslips in 96 well plates were incubated with FITC-labeled OSs (5×10^6 OSs in 40 μl/well, in excess of 10 OSs/RPE cell) in DMEM with 5% fetal bovine serum in the presence of lipids or ethanol solvent at a concentration of 1%. At the end of the incubation time, excess OSs were removed and cells were washed. To quench external OSs, samples were incubated with 0.4% trypan blue for 10 min, before washing and fixation in ice-cold methanol. Nuclei were labeled with 1 μg/ml propidium iodide. FITC and propidium iodide fluorescence of coverslips mounted on slides was quantified by fluorescence scanning on a STORM 860 scanner (Molecular Dynamics). Data were evaluated using Molecular Dynamics ImageQuaNT version 1.2 software. Samples were also evaluated by laser scanning confocal microscopy. Individual X-Y scans were acquired from representative fields. All studies included parallel control cytotoxicity and apoptosis assays to evaluate if exposures reduced cell viability. We did not observe toxicity of compounds or solvents on any of the RPE preparations when testing cell viability and signs of apoptosis by trypan blue dye exclusion and nuclear DNA fragmentation, respectively.

Light Exposure of Sprague-Dawley Rats and Retina Harvest

Weanling male Sprague-Dawley rats were obtained from Harlan Inc. (Indianapolis, IN) and maintained in a darkened room for 60 days. Animals were exposed to green light (~1200 lux; 200 microwatts/cm^2) for periods of either 1 or 4 h, as described previously (33), at which time animals were euthanized and retinas rapidly harvested as described (34). Excised retinas were immediately placed into argon-sparged saline (0.9%), supplemented with antioxidant mixture (100 μM butylated hydroxytoluene and 2 mM DTPA, pH 7) and rinsed of any free blood. Individual retinas were then rapidly submerged in 1-ml cryo vials filled with 0.75 ml of argon-sparged anti-oxidant mixture-containing saline, headspacepurged with argon, capped, snap frozen in liquid N_2, and then stored at −80 °C until analysis.

Separation of Phospholipids from Retina

To prevent artificial oxidation of retina, all procedures were performed rapidly within a dark room with dim red light. All glassware tubes and pipette tips were washed with nitric acid to remove trace transition metals, extensively rinsed with Chelex-treated water containing 1 μM DTPA, and then rinsed with pure Chelex-treated water. Plastic tips were further rinsed

in methanol and air-dried prior to use. All glassware was baked at 500 °C for 24 h to remove residual organics. Retinas were removed from the −80 °C freezer and thawed at 4 °C. Tissue was homogenized with a Teflon pestle in a form-fitting plastic vial with argon blanket. Vial contents were transferred to 10-ml threaded glass test tubes equipped with teflonlined caps, and then lipids within samples were extracted using the method of Bligh and Dyer (30) under argon after addition of 5 ng of DTPC as internal standard, followed by immediate HPLC with on-line electrospray ionization tandem mass spectrometry (LC/ESI/MS/MS) analysis. Extraction efficiencies of each of the oxPCs indicated (Fig. 1A) were determined using synthetic authentic oxPC species and the corresponding precursor (PA-PC, PL-PC, and DHA-PC) and DTPC as internal standard. After extraction, the amounts recovered were determined by LC/ESI/MS/MS.

Mass Spectrometric Analysis of Phospholipids

Lipid extracts were re-dissolved in methanol:water (90:10) and LC/ESI/MS/MS performed using a Prodigy ODS C18 column for separation of lipids and the HPLC solvent system described above. Mass spectrometric analyses were performed online using electrospray ionization tandem mass spectrometry in the positive ion, multiple reaction monitoring (MRM) mode (cone energy 30 V/collision energy 25 eV). The MRM transitions used to detect individual oxidized phospholipids were the mass to charge ratio (*m/z*) for the molecular cation $[M+H]^+$ and their daughter ion 184, the phosphatidylcholine group. Calibration curves for quantitative analyses of individual oxPC molecular species were constructed by mixing a fixed amount of internal standard (DTPC) into various amounts of authentic oxPC samples (35).

Nitrotyrosine Quantification

Protein-bound nitrotyrosine in retina was quantified by stable isotope dilution LC/MS/MS as previously described (36) on a triple quadrupole mass spectrometer (API 365, Applied Biosystems, Foster City, CA) with Ionics EP 10+ upgrade (Concord, Ontario, CA) interfaced to a Cohesive Technologies Aria LX Series HPLC multiplexing system (Franklin, MA). Synthetic $^{13}C_6$-labeled standard was added to delipidated tissue homogenates and used as internal standards for quantification of natural abundance analytes. Simultaneously, a universally labeled precursor amino acid, [$^{13}C_9$,$^{15}N_1$]tyrosine, was added. Proteins were hydrolyzed under argon atmosphere in methane sulfonic acid, and then samples were passed over mini solid-phase C18 extraction columns (Supelclean LC-C18-SPE minicolumn, 3 ml, Supelco, Inc., Bellefone, PA) prior to mass spectrometry analysis. Results are normalized to the content of the precursor amino acid tyrosine, which was monitored within the same injection. Intrapreparative formation of nitro[$^{13}C_9$,^{15}N]tyrosine was routinely monitored and negligible (*i.e.* ≪5% of the level of the natural abundance product observed) under the conditions employed.

Results

Evolution Profiles of Structurally Defined oxPCs from Light-exposed DHA-PC

We previously characterized a conserved high affinity CD36 binding motif in a family of oxidized choline glycerophospholipids derived from PAPC and PLPC ($oxPC_{CD36}$) consisting of an oxidatively truncated *sn*-2 acyl group with a terminal γ-hydroxy(or oxo)-α,β-unsaturated carbonyl (Fig. 1A) (25). According to mechanistic predictions, the oxidation of DHA-PC should produce compounds structurally analogous to these ligands (28). Photo-induced oxidation products of DHA-PC, however, have not yet been described. We synthesized the presumptive truncated peroxidation products of DHA-PC that might serve as CD36 ligands (see Fig. 1A for structures) and confirmed their structures by NMR and mass spectrometry (24, 28, 35). LC/ESI/MS/MS-based methods were then developed

for their simultaneous quantification (Fig. 1B). To test the hypothesis that these species are formed by photo-oxidation of DHA-PC, small unilamellar vesicles comprised of DHA-PC were either exposed to light (350 nm) or incubated in the dark and the evolution profiles of specific oxPC quantified by LC/ESI/ MS/MS (Fig. 1C). In buffer free of transition metal ions, DHA-PC vesicles maintained in the dark failed to generate significant levels of oxidation products. In marked contrast, irradiation with 350 nm light resulted in immediate oxPC production (Fig. 1C). HOHA-PC reached a maximum observed yield (1.3%) after 4 h and then started to decrease. Production of other species such as KOHA-PC, HHdiA-PC, KHdiA-PC, and OB-PC increased quickly during the first 4 h and subsequently slowed. Production of S-PC displayed an almost linear increase with time, and reached 1.7% yield after 28 h, suggesting that S-PC may be a final unhydrolyzed truncated product, and other oxPCs from DHA-PC apparently are further fragmented or oxidized into S-PC. Consistent with this hypothesis, light exposure to individual preparations of POPC vesicles containing 25 mol % of other DHA-PC oxidation products (*e.g.* HOHA-PC, KOHA-PC, HHdiA-PC, and KHdiA-PC) resulted in production of S-PC (data not shown).

oxPCs Formed during Photo-oxidation of DHA-PC Are High Affinity CD36 Ligands

The ability of DHA-PC derived oxPC to bind CD36 was first evaluated by competitive binding assays using the known CD36 ligand [^{125}I]NO_2-LDL and CD36 cDNA transfected 293 cells. Each synthetic lipid was mixed at 10 mol % within carrier POPC unilamellar vesicles. In contrast to vesicles containing native DHA-PC, γ-hydroxy-(oxo)-α,β-unsaturated oxPCs dose-dependently inhibited the binding of [^{125}I]NO_2-LDL to CD36 (Fig. 2A). Oxidized species possessing a terminal carboxylic acid moiety inhibited more effectively than those possessing a terminal aldehyde (HHdiA-PC *versus* HOHA-PC), and γ-keto compounds were more potent than γ-hydroxy compounds (KOHA-PC *versus* HOHA-PC), similar to prior structure/function studies observed with $oxPC_{CD36}$ derived from PLPC and PAPC (25, 26). The more terminally oxidized and truncated oxidation products of DHA-PC, S-PC and OB-PC, failed to significantly inhibit when presented at 10 mol % (Fig. 2A) but showed CD36 binding activity at higher levels (100 mol %, 20 μM lipids dissolved in phosphate-buffered saline buffer containing 10% ethanol), with S-PC binding more avidly than OB-PC relative to DHA-PC (Fig. 2B).

oxPCs Inhibit Uptake of OSs by RPE

Multiple oxPCs derived from DHA-PC, PLPC, and PAPC were tested for their ability to inhibit binding and internalization of isolated OSs by RPE cells in culture. The relatively non-oxidizable phospholipid, POPC, was used as a negative control. Because we suspected that some oxPCs might be enzymatically hydrolyzed into lyso-PC in cell culture, the activity of lyso-PC was also tested. RPE-J cells were incubated with FITC-labeled OSs with or without the presence of the indicated phospholipids. At 1.5 h of OSs incubation RPE-J cells bound FITC-OS, but less than 10% were internalized. As expected, none of the $oxPC_{CD36}$ examined had an appreciable effect on binding of OSs to RPE-J cells (Fig. 3, $p > 0.05$ for all lipids *versus* control). At 1.5 h OB-PC, S-PC, lyso-PC, and POPC showed no effect on uptake of OS, whereas all γ-hydroxy(oxo)-α,β-unsaturated oxPCs evaluated, including the ketoaldehydes (KODA-PC, KOOA-PC, and KOHA-PC), ketoacids (KDdiA-PC, KOdiA-PC, KHdiA-PC), and hydroxy acid, inhibited uptake by 10–20% ($p < 0.05$, Fig. 3, *middle panel*). After longer incubation (3.5 h) the most active CD36 ligands, such as KDdiA-PC, inhibited uptake by ~50% ($p < 0.05$), whereas POPC and lyso-PC, which may be a hydrolysis product of oxPCs, had little effect. Parallel control studies demonstrated no toxicity of oxPC exposure to RPE-J cells as assessed by trypan blue dye exclusion and nuclear DNA fragmentation (data not shown). Collectively, these results confirm that the functional groups at the *sn*-2 position of the oxPCs are important for RPE-mediated internalization of OS.

CD36 Recognition of Structurally Specific Oxidized Phospholipids and RPE Phagocytosis of OS

To evaluate the role of CD36 in RPE recognition of oxidized PC species within isolated OS, primary cultures of RPE were prepared from wild-type and CD36 null mice. First, we used our established phagocytosis assay to compare FITC-OSs uptake by wild-type and CD36 null RPE. While at the end point CD36 null RPE cells internalized similar numbers of OSs as wild-type RPE (Fig. 4, A and B), there was a difference in the lag period prior to phagocytosis in wild-type *versus* CD36 null cells (CD36 null cells demonstrated longer lag period, data not shown). CD36 null and WT RPE demonstrated no detectable differences in either expression or localization of the tight junction marker ZO-1, as observed by fluorescence microscopy (Fig. 4, C and D). Similarly, comparable cell morphology and pigmentation were observed in wild-type *versus* CD36 null RPE by transmission white light microscopy (Fig. 4, E and F). The overlay of tight junctions (*green*), cell nuclei (*red*), and transmitted light (*blue*) in Fig. 4(G and H) further confirms that RPE cells from both genotypes had similar size, morphology, pigmentation, and epithelial organization.

We next compared sensitivity of OSs phagocytosis by wild-type and CD36 null RPE to competition by CD36 phospholipid ligands. Although POPC and lyso-PC showed little effect on OS uptake by RPE, all $oxPC_{CD36}$ examined (KDdiA-PC, KODA-PC, KOdiA-PC, KOOA-PC, KHdiA-PC, and KOHA-PC) significantly inhibited OS uptake by RPE from wild-type mice but not in RPE isolated from CD36 null mice (Fig. 5). These results are consistent with the hypothesis that CD36 partially contributes to OS phagocytosis through recognition of structurally specific oxPCs on the surface of OSs.

$oxPC_{CD36}$s Are Present in Rat Retina, and Their Production Is Promoted by Physiological Light Exposure

It has been suggested that light exposure may initiate the peroxidation of polyunsaturated fatty acids such as arachidonic acid (37) and DHA in retina (38), although we are unaware of any direct demonstration of structurally defined phospholipid oxidation products formed within retina *in vivo* following light exposure. We hypothesized that the light-triggered peroxidation of the phosphocholine esters of polyunsaturated fatty acids (PAPC, PLPC, and DHA-PC) in retina would produce oxPCs, including some that have already been detected *in vitro* or in other biological systems such as atherosclerotic lesions (26). To examine if oxPCs are present in intact retinas and if light exposure promotes their production *in vivo*, retinas harvested from albino rats with or without light treatment were analyzed by LC/ESI/MS/MS. Three groups of rats (eight in each group) were raised in the dark for 60 days, and two groups were then treated with green light (550 ± 75 nm) for 1 and 4 h, respectively. The intensity of light used, ~200 microwatts/cm^2 corneal irradiation, represents ~2-to 3-fold higher level than that of typical ambient laboratory conditions. To prevent *ex vivo* lipid peroxidation retinas were harvested immediately in the dark under continuously argon-sparged buffer supplemented with anti-oxidants, and lipids were extracted and preserved in amber-walled vials under inert atmosphere with anti-oxidants present and then rapidly analyzed utilizing LC/ESI/MS/MS. Eighteen distinct oxPCs (see Fig. 1A for structures) and their corresponding precursors, PLPC, PAPC, and DHA-PC, were monitored simultaneously. Eight oxPCs species were reproducibly detected in dark-adapted rat retinas. Among the oxPCs derived from PLPC, ON-PC and A-PC were detected (Fig. 6); among the oxPCs derived from PAPC, OV-PC and G-PC were detected (Fig. 6A); and among the oxPCs derived from DHA-PC, OB-PC, S-PC, KOHA-PC, and HOHA-PC were detected (Fig. 6B). Retention time and characteristic parent ion → daughter ion transitions of each compound were collectively used to identify the oxPC species.

Quantitative data for each detected oxPC within individual retina are presented in Fig. 7. The content of each oxPC is reported as the ratio of oxPC to its precursor (*e.g.* HOHA-PC/DHA-PC, millimole/mol). Light exposure significantly increased the levels of most of the oxPC monitored, including OB-PC, HOHA-PC, KOHA-PC, OV-PC, G-PC, KOOA-PC, A-PC, and ON-PC ($p < 0.05$ each). The failure to detect some oxPCs may be a consequence of either their low abundances, further oxidation into alternative species, or covalent adduction to nucleophilic groups such as retinal proteins. As observed with the *in vitro* experiments, the more terminal oxidation cleavage products, including simple aldehydes (ON-PC, OV-PC, and OB-PC) and acids (A-PC, G-PC, and S-PC), were the most abundant species detected, and they collectively accounted for in excess of 15–20 mol % of their corresponding unoxidized precursors.

In a final series of studies, the role of nitric oxide (NO)-derived oxidants as a potential participant in retinal oxidant stress following light exposure was explored, because recent studies suggest that enhanced nitrative stress may participate in retinal pathologies, such as age-related macular degeneration (39). Stable isotope dilution tandem mass spectrometry-based analyses of retinal proteins confirmed time-dependent increases in retinal protein nitrotyrosine content following light exposure (Fig. 8).

Discussion

Coordinated phagocytosis of OSs by RPE is necessary for maintenance of normal retinal function. Rodents with null mutations in the gene for the OS-RPE adhesion receptor integrin $\alpha_v\beta_5$ or the tyrosine kinase receptor Mer lose capacity for OSs phagocytosis and develop retinal degeneration and blindness (6, 40–42). Similarly, mutations in Mer have been associated with hereditary retinal degeneration syndromes in humans (43). Previous studies exploring the potential role of the class B scavenger receptor CD36 in RPE-mediated phagocytosis reveal that blockade of CD36 *in vitro* inhibits OSs phagocytosis and that clustering of CD36 by multivalent ligands provides a phagocytic signal to RPE (13,15,16). Analysis of CD36-deficient mice and rats, however, did not reveal retinal pathology under standard vivarium conditions. However, rats that harbor a deletion variant in the scavenger receptor CD36 were found to be more sensitive to intense light-induced retinal damage (44). Based on these data we concluded that CD36 signaling is not essential for RPE phagocytosis under basal conditions, but under conditions where oxidative stress is increased we hypothesize that CD36 may be involved in OS clearance. Defects in this pathway may relate to the increased risk of age-related macular degeneration reported in conditions with heightened oxidative stress, such as cigarette smoking (45).

Although significant progress has been made in identifying RPE receptors for shed OSs, little is known of the retinal ligands for these receptors. Because all of the putative OS phagocytic receptors are constitutively expressed by RPE, it is reasonable to speculate that alterations of surface components of OSs occur commensurate with shedding and that these changes generate recognition and internalization signals for the phagocytic receptors. In the current study we demonstrate that structurally defined oxidized choline glycerophospholipids play a role in RPE recognition of OSs via interaction with CD36. Oxidized phospholipids derived from the common retinal lipid DHA, similar to their structural analogs derived from arachidonic acid and linoleic acid (25, 26), effectively competed with oxLDL for binding to CD36, and inhibited uptake of OSs by RPE. Furthermore, studies using primary RPE isolated from mice showed a clear phenotypic difference between cells from CD36 null and wild-type C57Bl animals; oxidized phospholipids inhibited OS uptake by wild-type cells but not by CD36 deficient cells. Finally, our studies of dark-adapted rats exposed to brief intense light intervals showed that

oxidative stress induced by light exposure changed the content of oxidized phospholipids in the retina, increasing expression of potential CD36 ligands.

Although oxidative alterations of surface components of OSs occur with shedding, generating CD36 recognition and internalization signals, an intriguing question that remains is how CD36 actually recognizes the structurally defined oxPC formed with apparent specificity. In prior structure function studies, only modest alterations to the core structural motif identified as conferring high affinity CD36 recognition (a PC harboring an oxidatively truncated *sn*-2 acyl group with a terminal γ-hydroxy(or oxo)-α,β-unsaturated carbonyl) resulted in marked diminution in binding affinity. For example, either moving the γ-hydroxy group only one methylene down to the δ position, or dehydrating the oxPC at the γ-hydroxy position, resulted in structural analogs that completely lacked CD36-binding activity (25). These results suggest specific structural features of oxPC may be recognized by CD36 on the surface of a membrane. Phospholipids adopt distinct aggregate liquid crystalline structures (mesomorphic forms). By performing binding studies under conditions where oxPC species were incorporated at only trace levels into a lamellar (bilayer) phase preferring PC under the conditions examined (POPC), we attempted to minimize gross alterations in membrane molecular packing that might occur from “patches” of oxPC within PC bilayers. We anticipate that both the membrane molecular dynamics and phospholipid conformation in the immediate vicinity of the more polar oxPC species will be altered and can only speculate that the structure adopted by these species facilitates the observed enhanced binding affinity with CD36. Further study of both oxPC and CD36 protein conformations at the site of interactions are of interest.

The physiological relevance of the present findings are suggested by the observation of comparable levels of oxidized phospholipids being produced within retina following light exposure (collectively in excess of 10 mol % of parental choline glycerophospholipid molecular species) and levels of structurally distinct oxidized phospholipids incorporated within membranes sufficient to promote CD36 recognition (*e.g.* 10 mol % was used in competition studies shown in Fig. 2A). Moreover, the intensity of light used in this study, ~200 microwatts/cm^2 corneal irradiation, is only 2- to 3-fold higher than that found in the laboratory or typical animal rearing facilities. These light levels have been shown both to induce OS shedding and to increase phagosome counts in the RPE (4) and to result in photoreceptor cell death (38,46). Thus, the present data suggest that, under conditions of oxidant stress, oxidized phospholipids may serve as a physiological signal for RPE cells via CD36, leading to increased OS turnover in retina upon light damage when the capacity of the normal αvβ5-MerTK clearance pathway may not suffice. The present studies may also provide a molecular mechanism for the prior observation that spontaneously hypertensive rats are more sensitive to light-induced retinal damage (44), a rat strain whose phenotype is now recognized to be conferred by a specific deletion variant within the CD36 gene (46).

The mechanisms by which light induces lipid oxidation in the retina is still unclear. A recent study demonstrated that rhodopsin is essential for light-induced retinal degeneration. Slowing down regeneration of 11-*cis*-retinal, a key material for the regeneration of rhodopsin, had protective effects against photo-damage (47). Rhodopsin may mediate damage by photochemical reactions. Both blue light (403 nm) and green light (550 nm) can bleach rhodopsin, producing all-*trans*-retinal, a well known photosensitizer (48). Retinal can be excited to its triplet state, the high energy of which can be transferred to molecular oxygen to produce singlet oxygen (49) and superoxide (50). Other photo-sensitizers have also been identified. Lipofuscin, a heterogeneous group of complex, lipid-protein aggregates, which fluoresce upon irradiation with UV and short wavelength light, has been shown to generate reactive oxygen species such as singlet oxygen, hydrogen peroxide, and lipid hydroperoxide (51, 52). The green Plexiglas® filter used in the present studies filters

out all UV light while transmitting 490–580 nm light (53), consistent with a potential role for rhodopsin photobleaching within OSs as the initiator of photo damage and the oxidative lipid changes found.

In our parallel studies of protein oxidation products in the light-stressed retina we found increased levels of nitrotyrosine, suggesting that increased nitrative stress may also contribute as a potential mechanism for initiation of lipid peroxidation. The formation of nitrotyrosine in retina strongly supports the hypothesis that peroxynitrite ($ONOO^-$) (54), the reaction product of both NO and superoxide, was generated. Peroxynitrite decomposition produces nitrogen dioxide radical and hydroxyl radical, which can nitrate tyrosine and initiate lipid peroxidation (55). NO is synthesized from arginine by nitric-oxide synthasecatalyzed reactions (56), and nitric-oxide synthases have been shown to be required for light-induced photoreceptor apoptosis (57). It is interesting to note that inhibition of nitric-oxide synthases has been shown to protect rats against light-induced retinal degeneration (58).

In sum, the data reported herein identify a mechanism by which CD36 ligands can be generated in the retina in response to oxidative and photo-stress. Using synthetic and analytic techniques coupled with study of primary RPE cells from genetically modified mice, we demonstrated that structurally defined oxidized choline glycerophospholipid molecular species both serve as CD36 ligands during OS uptake and are generated within the retinas of light-stressed animals. These data suggest a potential physiological role for CD36 in RPE turnover of light-damaged OSs under conditions of oxidative stress.

References

1. Young RW, Bok D. J Cell Biol. 1969; 42:392–403. [PubMed: 5792328]
2. LaVail MM. Science. 1976; 194:1071–1074. [PubMed: 982063]
3. Fliesler SJ, Anderson RE. Prog Lipid Res. 1983; 22:79–131. [PubMed: 6348799]
4. Blanks JC, Pickford MS, Organisciak DT. Invest Ophthalmol Vis Sci. 1992; 33:2814–2821. [PubMed: 1526731]
5. Watson CL, Gold MR. Circ Res. 1997; 81:387–395. [PubMed: 9285641]
6. Nandrot EF, Kim Y, Brodie SE, Huang X, Sheppard D, Finnemann SC. J Exp Med. 2004; 200:1539–1545. [PubMed: 15596525]
7. Finnemann SC, Bonilha VL, Marmorstein AD, Rodriguez-Boulan E. Proc Natl Acad Sci U S A. 1997; 94:12932–12937. [PubMed: 9371778]
8. Vollrath D, Feng W, Duncan JL, Yasumura D, D'Cruz PM, Chappelow A, Matthes MT, Kay MA, LaVail MM. Proc Natl Acad Sci U S A. 2001; 98:12584–12589. [PubMed: 11592982]
9. Hall MO, Prieto AL, Obin MS, Abrams TA, Burgess BL, Heeb MJ, Agnew BJ. Exp Eye Res. 2001; 73:509–520. [PubMed: 11825022]
10. Hall MO, Obin MS, Prieto AL, Burgess BL, Abrams TA. Exp Eye Res. 2002; 75:391–400. [PubMed: 12387786]
11. Hall MO, Abrams T. Exp Eye Res. 1987; 45:907–922. [PubMed: 2828096]
12. Chaitin MH, Hall MO. Invest Ophthalmol Vis Sci. 1983; 24:812–820. [PubMed: 6345445]
13. Ryeom SW, Sparrow JR, Silverstein RL. J Cell Sci. 1996; 109:387–395. [PubMed: 8838662]
14. Boyle D, Tien LF, Cooper NG, Shepherd V, McLaughlin BJ. Invest Ophthalmol Vis Sci. 1991; 32:1464–1470. [PubMed: 1901835]
15. Ryeom SW, Silverstein RL, Scotto A, Sparrow JR. J Biol Chem. 1996; 271:20536–20539. [PubMed: 8702796]
16. Finnemann SC, Silverstein RL. J Exp Med. 2001; 194:1289–1298. [PubMed: 11696594]
17. Silverstein RL, Febbraio M. Curr Opin Lipidol. 2000; 11:483–491. [PubMed: 11048891]
18. Daviet L, McGregor JL. Thromb Haemost. 1997; 78:65–69. [PubMed: 9198129]

19. Nozaki S, Kashiwagi H, Yamashita S, Nakagawa T, Kostner B, Tomiyama Y, Nakata A, Ishigami M, Miyagawa J, Kameda-Takemura K, Kurata Y, Matsuzawa Y. J Clin Investig. 1995; 96:1859–1865. [PubMed: 7560077]
20. Jimenez B, Volpert OV, Crawford SE, Febbraio M, Silverstein RL, Bouck N. Nat Med. 2000; 6:41–48. [PubMed: 10613822]
21. Febbraio M, Abumrad NA, Hajjar DP, Sharma K, Cheng W, Pearce SF, Silverstein RL. J Biol Chem. 1999; 274:19055–19062. [PubMed: 10383407]
22. Podrez EA, Febbraio M, Sheibani N, Schmitt D, Silverstein RL, Hajjar DP, Cohen PA, Frazier WA, Hoff HF, Hazen SL. J Clin Invest. 2000; 105:1095–1108. [PubMed: 10772654]
23. Febbraio M, Hajjar DP, Silverstein RL. J Clin Invest. 2001; 108:785–791. [PubMed: 11560944]
24. Sun M, Deng Y, Batyreva E, Sha W, Salomon RG. J Org Chem. 2002; 67:3575–3584. [PubMed: 12027667]
25. Podrez EA, Poliakov E, Shen Z, Zhang R, Deng Y, Sun M, Finton PJ, Shan L, Gugiu B, Fox PL, Hoff HF, Salomon RG, Hazen SL. J Biol Chem. 2002; 277:38503–38516. [PubMed: 12105195]
26. Podrez EA, Poliakov E, Shen Z, Zhang R, Deng Y, Sun M, Finton PJ, Shan L, Febbraio M, Hajjar DP, Silverstein RL, Hoff HF, Salomon RG, Hazen SL. J Biol Chem. 2002; 277:38517–38523. [PubMed: 12145296]
27. Gu X, Meer SG, Miyagi M, Rayborn ME, Hollyfield JG, Crabb JW, Salomon RG. J Biol Chem. 2003; 278:42027–42035. [PubMed: 12923198]
28. Gu X, Sun M, Gugiu B, Hazen S, Crabb JW, Salomon RG. J Org Chem. 2003; 68:3749–3761. [PubMed: 12737551]
29. Deng Y, Salomon RG. J Org Chem. 1998; 63:7789–7794.
30. Bligh EG, Dyer WJ. Can J Biochem Physiol. 1959; 37:911–917. [PubMed: 13671378]
31. Nabi IR, Mathews AP, Cohen-Gould L, Gundersen D, Rodriguez-Boulan E. J Cell Sci. 1993; 104:37–49. [PubMed: 8383696]
32. Finnemann SC. EMBO J. 2003; 22:4143–4154. [PubMed: 12912913]
33. Delmelle M, Noell WK, Organisciak DT. Exp Eye Res. 1975; 21:369–380. [PubMed: 1218544]
34. Organisciak DT, Darrow RM, Barsalou L, Kutty RK, Wiggert B. Invest Ophthalmol Vis Sci. 2000; 41:3694–3701. [PubMed: 11053264]
35. Sun, M. Thesis, Synthetic and Mechanistic Studies of Lipid Peroxidation in Vitro and in Vivo. Case Western Reserve University; Cleveland, OH: 2003. p. 262-282.
36. Nicholls SJ, Shen Z, Fu X, Levison BS, Hazen SL. Methods Enzymol. 2005; 396:245–266. [PubMed: 16291237]
37. Pautler EL. Curr Eye Res. 1994; 13:687–695. [PubMed: 7805400]
38. Organisciak DT, Wang HM, Li ZY, Tso MO. Invest Ophthalmol Vis Sci. 1985; 26:1580–1588. [PubMed: 4055290]
39. Miyagi M, Sakaguchi H, Darrow RM, Yan L, West KA, Aulak KS, Stuehr DJ, Hollyfield JG, Organisciak DT, Crabb JW. Mol Cell Proteomics. 2002; 1:293–303. [PubMed: 12096111]
40. Edwards RB, Szamier RB. Science. 1977; 197:1001–1003. [PubMed: 560718]
41. Scott RS, McMahon EJ, Pop SM, Reap EA, Caricchio R, Cohen PL, Earp HS, Matsushima GK. Nature. 2001; 411:207–211. [PubMed: 11346799]
42. Mullen RJ, LaVail MM. Science. 1976; 192:799–801. [PubMed: 1265483]
43. Gal A, Li Y, Thompson DA, Weir J, Orth U, Jacobson SG, Apfelstedt-Sylla E, Vollrath D. Nat Genet. 2000; 26:270–271. [PubMed: 11062461]
44. Li S, Lam TT, Fu J, Tso MO. Arch Ophthalmol. 1995; 113:521–526. [PubMed: 7710404]
45. Zarbin MA. Arch Ophthalmol. 2004; 122:598–614. [PubMed: 15078679]
46. Pravenec M, Landa V, Zidek V, Musilova A, Kazdova L, Qi N, Wang J, St Lezin E, Kurtz TW. Physiol Res. 2003; 52:681–688. [PubMed: 14640889]
47. Grimm C, Wenzel A, Hafezi F, Yu S, Redmond TM, Reme CE. Nat Genet. 2000; 25:63–66. [PubMed: 10802658]

48. Bensasson, RV.; Land, EJ.; Truscott, TG. Excited States and Free Radicals in Biology and Medicine: Contributions from Flash Photolysis and Pulse Radiolysis. Oxford University Press; Oxford, New York: 1993. p. 128-136.

49. Rozanowska M, Wessels J, Boulton M, Burke JM, Rodgers MA, Truscott TG, Sarna T. Free Radic Biol Med. 1998; 24:1107–1112. [PubMed: 9626564]

50. Dillon J, Gaillard ER, Bilski P, Chignell CF, Reszka KJ. Photochem Photobiol. 1996; 63:680–685. [PubMed: 8628760]

51. Rozanowska M, Jarvis-Evans J, Korytowski W, Boulton ME, Burke JM, Sarna T. J Biol Chem. 1995; 270:18825–18830. [PubMed: 7642534]

52. Gaillard ER, Atherton SJ, Eldred G, Dillon J. Photochem Photobiol. 1995; 61:448–453. [PubMed: 7770505]

53. Organisciak DT, Winkler BS. Prog Ret Eye Res. 1994; 13:1–29.

54. Ischiropoulos H, Zhu L, Chen J, Tsai M, Martin JC, Smith CD, Beckman JS. Arch Biochem Biophys. 1992; 298:431–437. [PubMed: 1416974]

55. Beckman JS, Beckman TW, Chen J, Marshall PA, Freeman BA. Proc Natl Acad Sci U S A. 1990; 87:1620–1624. [PubMed: 2154753]

56. Palmer RM, Ashton DS, Moncada S. Nature. 1988; 333:664–666. [PubMed: 3131684]

57. Donovan M, Carmody RJ, Cotter TG. J Biol Chem. 2001; 276:23000–23008. [PubMed: 11278285]

58. Goureau O, Jeanny JC, Becquet F, Hartmann MP, Courtois Y. Neuroreport. 1993; 5:233–236. [PubMed: 7507723]

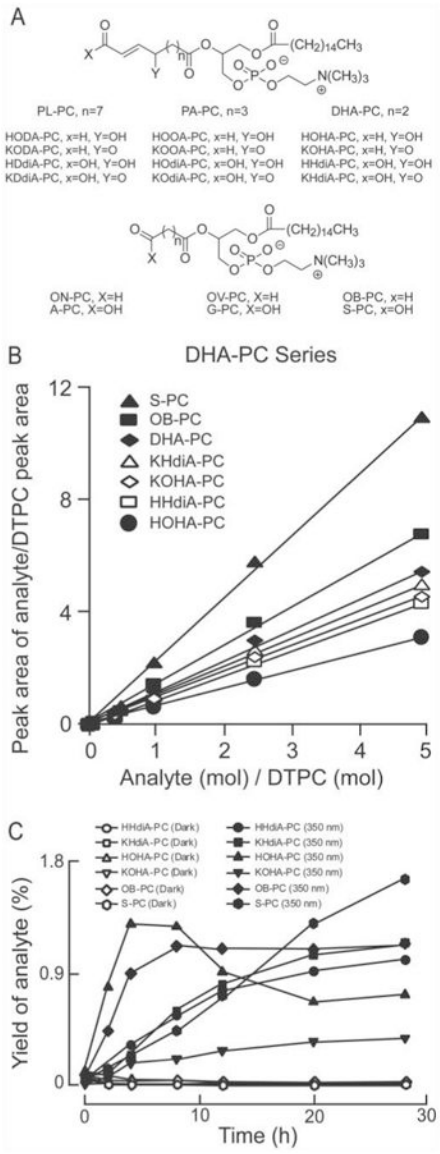

Figure 1. Structures of oxidatively truncated phospholipids produced from PL-PC, PA-PC, and DHA-PC

A, the compounds generated from different precursors are similar except for the number of methylene groups on the truncated oxidized fatty acid esterified to the *sn*-2 position of lyso-PC. *B*, standard curves for the quantification of the indicated oxPC were generated using known quantities of synthetic standards for each oxPC, and afixed amount of DTPCas internal standard. *C*, evolution profile of oxPCs from DHA-PC irradiated with 350 nm light. Quantification was achieved with LC/ESI/MS/MS. Yields were calculated by dividing the amount of each analyte by the amount of starting DHA-PC. Data are the average of two sets of independent experiments.

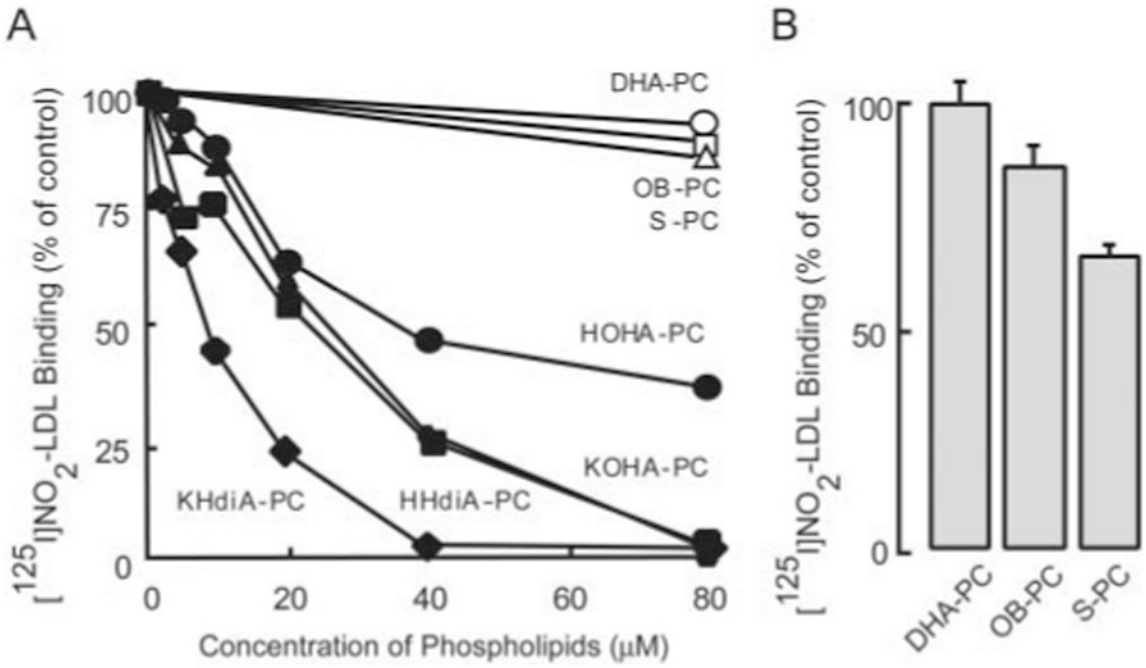

Figure 2. Synthetic oxPCs, with *sn*-2-esterified oxidized fatty acids possessing *γ*-hydroxy(oxo)-*α,β*-unsaturated carbonyl groups, inhibit oxidized LDL binding to CD36

A, [^{125}I]NO_2-LDL (5 μg/ml), a known ligand for CD36, was incubated with 293 cells stably transfected with human CD36 cDNA or vector-transfected control cells for 2 h at 4 °C in DMEM in the presence of small unilamellar vesicles comprised of 10 mol % of the indicated oxPC within POPC at the indicated total phospholipid concentrations. CD36-specific binding of [^{125}I]NO_2-LDL was then assessed as described under "Experimental Procedures." *B*, [^{125}I]NO_2-LDL binding as in A in the presence of competitor small unilamellar vesicles (20 μM total lipid) composed of the indicated pure oxPCs.

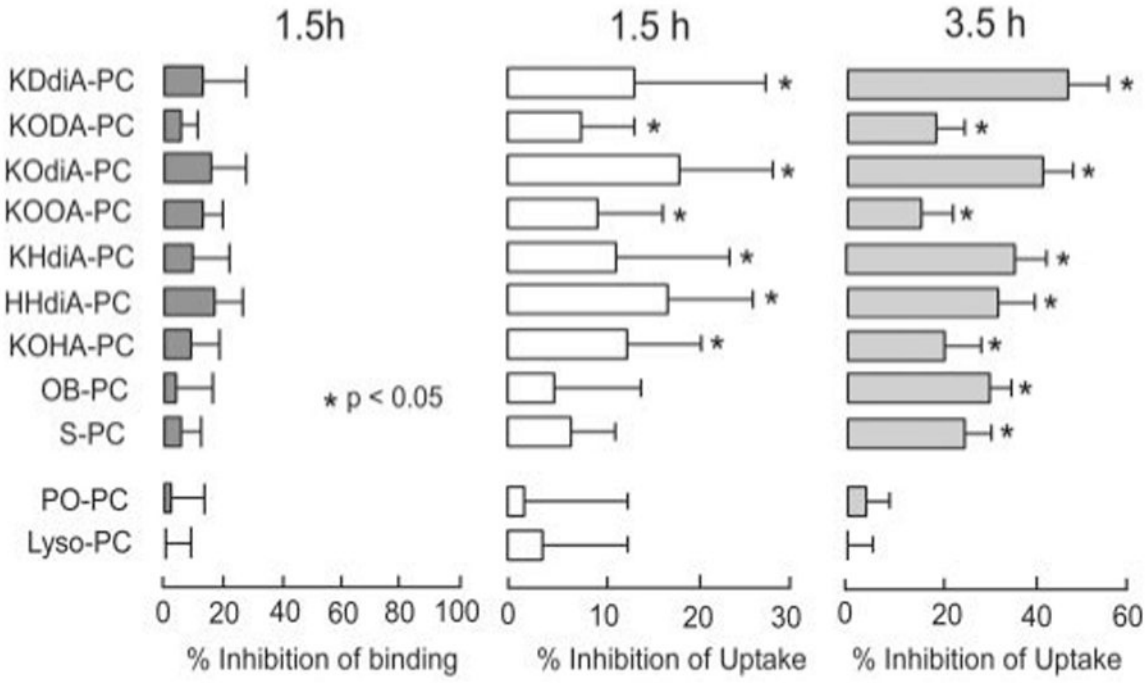

Figure 3. oxPCs inhibit uptake of OSs by RPE-J cells

Binding of FITC-OSs by RPE-J cells was not significantly inhibited by the presence of specific lipids after 1.5 h of incubation (*left panel*). OSs uptake by RPE-J cells after 1.5 h (*middle panel*) and 3.5 h (*right panel*) was significantly inhibited by specific oxidized lipids. In all studies lipid concentrations were 20 μM. Values are mean ± S.D. of triplicate experiments in each treatment. The *p* value was calculated against control (ethanol only).

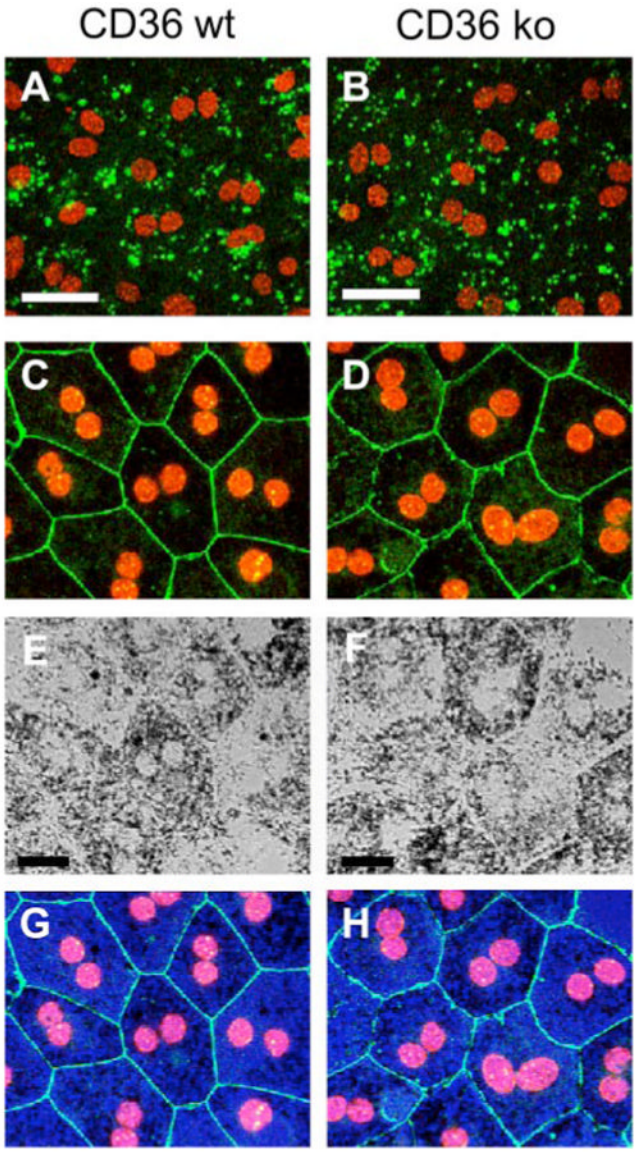

Figure 4. Wild-type and CD36 null RPE cells have similar morphology and phagocytic capacity

A and *B*, primary RPE derived from wild-type C57Bl mice (*CD36 wt*) or CD36 null mice (*CD36 ko*) were fed excess FITC-OSs for 1.5 h. Single x-y confocal scans of FITC-OSs (*green*) of representativefields were acquired in the samefocal plane as RPE cell nuclei (*red*). Perinuclear localization indicated that the FITC-OSs had been internalized by the cells. Cells from both genotypes internalized similar numbers of FITC-OS. *Scale bars* are 40 μm. *C* and *D*, primary RPE from CD36 wild-type (*C*) and CD36 null (*D*) mice were labeled with ZO-1 antibody (*green*) and nuclei stain (*red*). Maximal confocal projections of representative fields are shown. *Scale bars* are 20 μm. *E* and *F*, transmission light microscopy of the same fields as *C* and *D* showed that CD36 null RPE retains normal pigmentation. *G* and *H*, the *merged image* of *C* and *E* for CD36 wild-type (*G*) and *D* and *F* for CD36 null (*H*) shows overlay of junctions (*green*), cell nuclei (*red*), and pigmentation (*blue*), further confirming similar epithelial morphology of CD36 null and wild-type RPE.

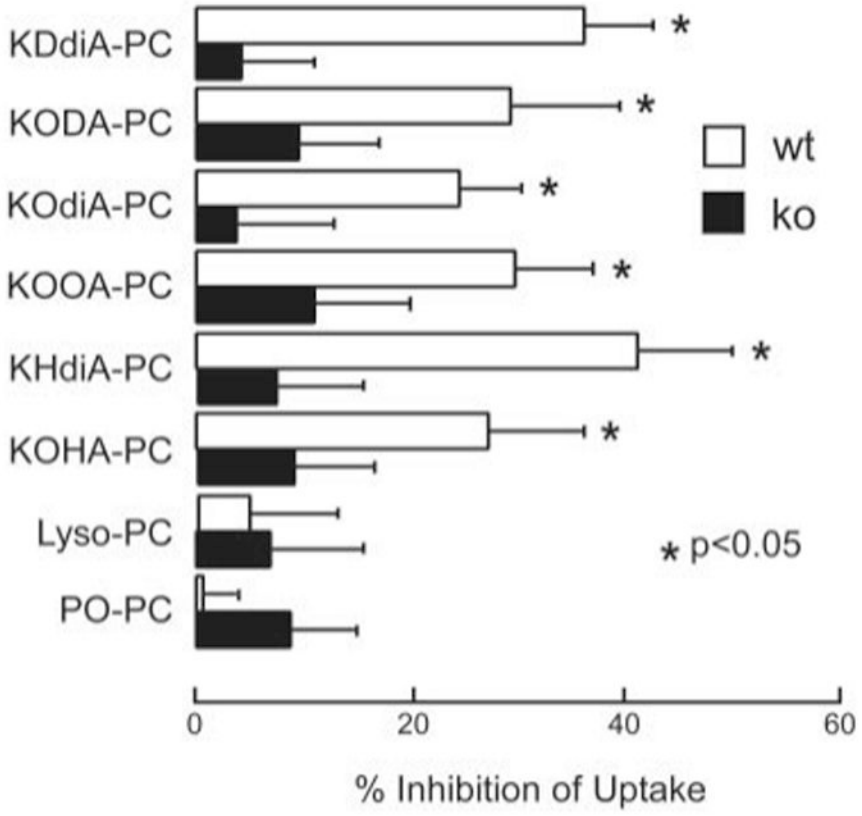

Figure 5. oxPCs inhibit OSs uptake by wild-type but not CD36 null RPE

oxPCs at 20 μm were incubated with primary RPE from wild-type C57Bl mice (*wt*) or CD36 null mice (*ko*) prior to addition of FITC-OSs for 1.5 h. Intact PC (*POPC*) and hydrolyzed oxPC (*lyso-PC*) had no effect on uptake by cells from either mouse strain, whereas the oxPC species significantly inhibited uptake by wt, but not ko cells. Values are mean ± S.D. of triplicate experiments in each treatment. The *p* value was calculated against carrier (ethanol) control.

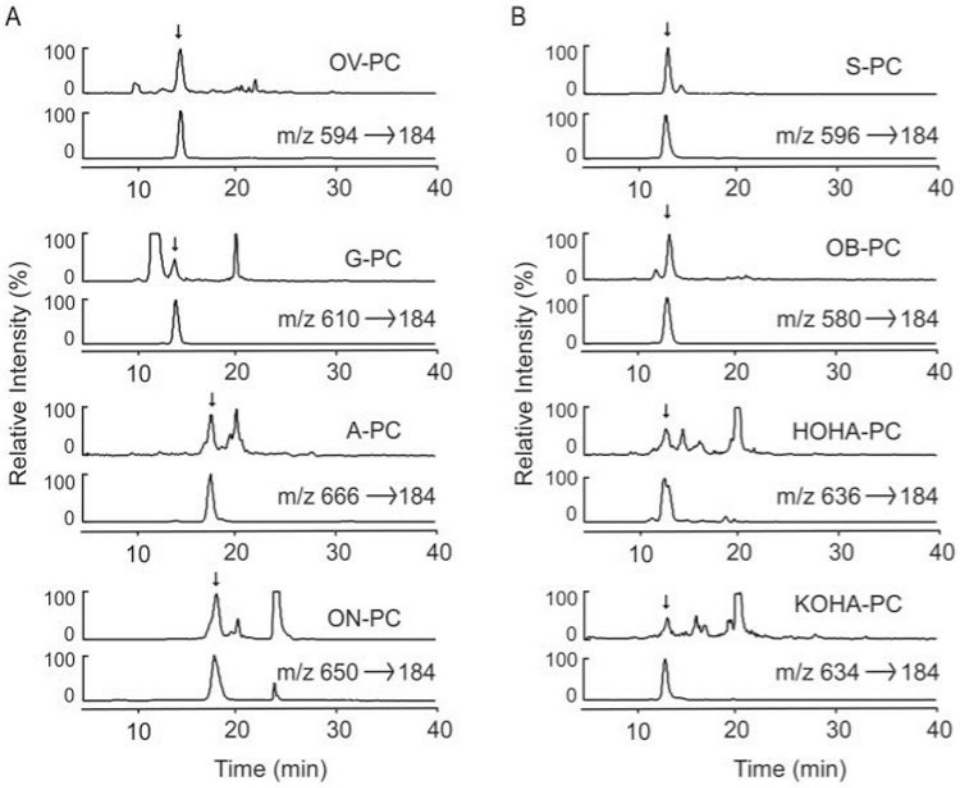

Figure 6. ***In vivo*** **detection of oxPCs from rat retinas by LC/MS/MS**

A, PA-PC and PL-PC-derived species. oxPCs were extracted from the retina of weaning male Sprague-Dawley rats exposed to green light for 4 h. The oxPCs were fractionated by a reversed-phase HPLC column and quantified using online ESI/MS/MS. Chromatograms of each oxPC extracted from retina obtained using LC/MS/MS with MRM are shown. The *upper trace* in each panel represents the ion current of MRM analysis of specific parent/daughter transition of indicated oxPCs in retina extract. The *lower panel* illustrates the ion current of MRM analysis of specific parent/daughter transition of the indicated synthetic oxPC standard. *B*, DHA-PC-derived species.

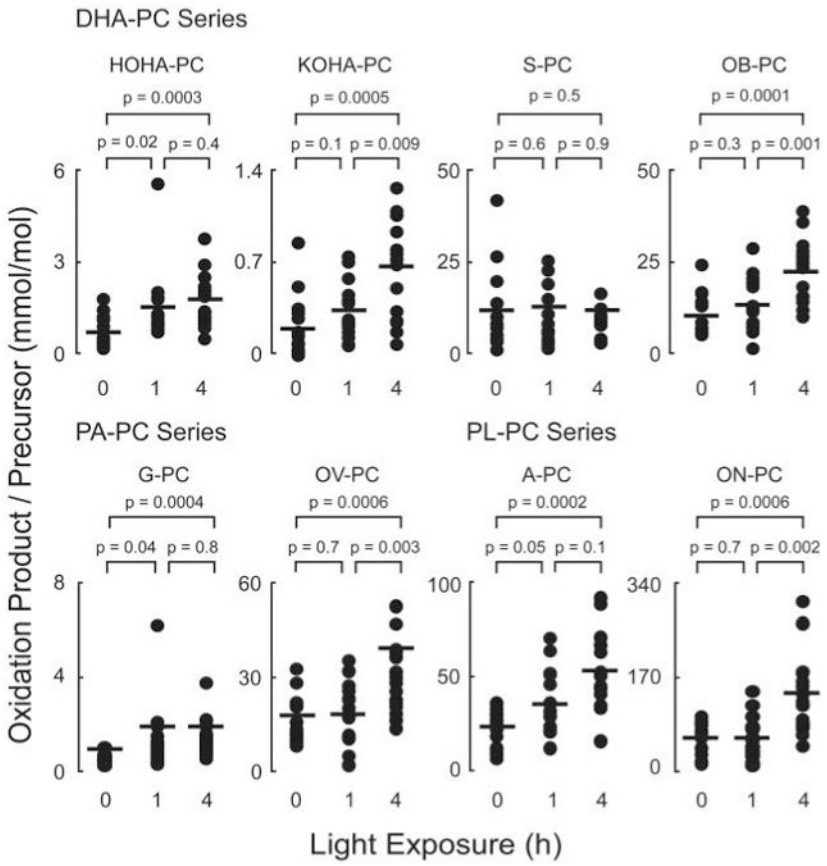

Figure 7. Light exposure increases retinal levels of oxPCs

Retinal lipids of rats with or without acute green light exposure were extracted and analyzed as described in Fig. 6. Dark-adapted animals were considered as 0-h light exposure. oxPCs observed are normalized to the level of the precursors. Each *dot* represents the measured level of an oxPC in a retina. There are sixteen retinas in each group. The *p* values were obtained by using Student's *t* test.

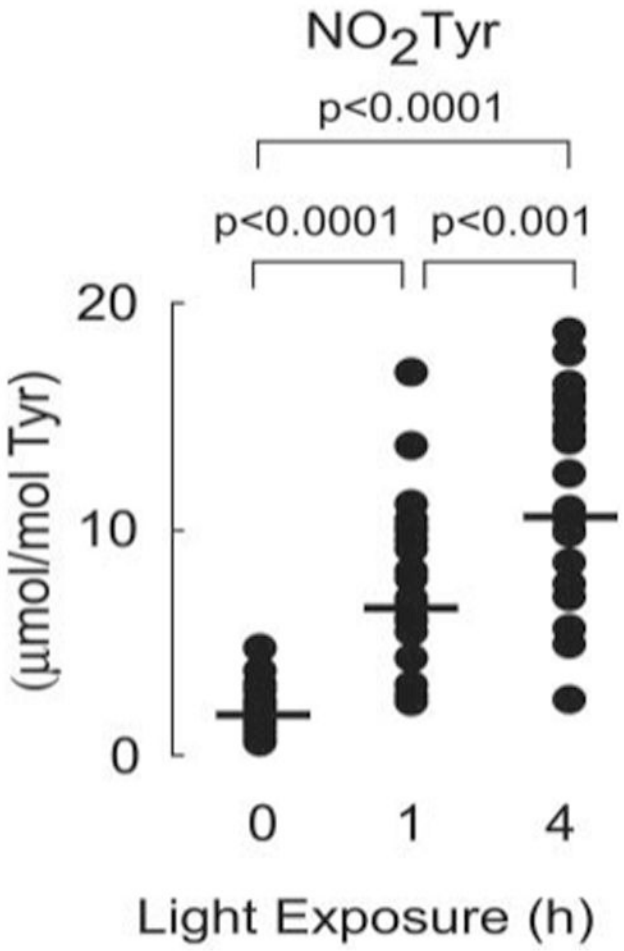

Figure 8. Light exposure increases retinal levels of nitrotyrosine

Protein-bound nitrotyrosine levels of rat retina with or without acute green light exposure were determined in delipidated protein extracts of retina described in Fig. 6. Dark-adapted animals were considered as 0-h light exposure. Retinal protein nitrotyrosine contents are normalized to the level of the precursor amino acid, tyrosine. Each *dot* represents the measured level of nitrotyrosine in a retina. There are sixteen retinas in each group. The *p* values were obtained by using Student's *t* test.